

Supporting information for

Solvent-mediated subcomponent self-assembly of covalent metallacycles for hierarchical porous materials synthesis

Zhi-Wei Li,^{*ab} Anlian Huang,^b Zhenguo Wang,^b Rui Gao,^b Bang Lan,^{*a} Guosheng Chen,^{*b} and Gangfeng Ouyang^b

a, Northeast Guangdong Key Laboratory of New Functional Materials, School of Chemistry and Environment, Jiaying University, Meizhou, 514015, China.

b, MOE Key Laboratory of Bioinorganic and Synthetic Chemistry, GBRCE for Functional Molecular Engineering, School of Chemistry, IGCME, Sun Yat-Sen University, Guangzhou 510275, China.

Contents

1. Materials and methods.....	3
2. Synthesis	4
3. High-resolution MS analysis.....	14
4. Single-crystal X-ray analysis.	19
5. Hirshfeld surface analysis.....	21
6. Characterization of mMOF-1.....	25

1. Materials and methods

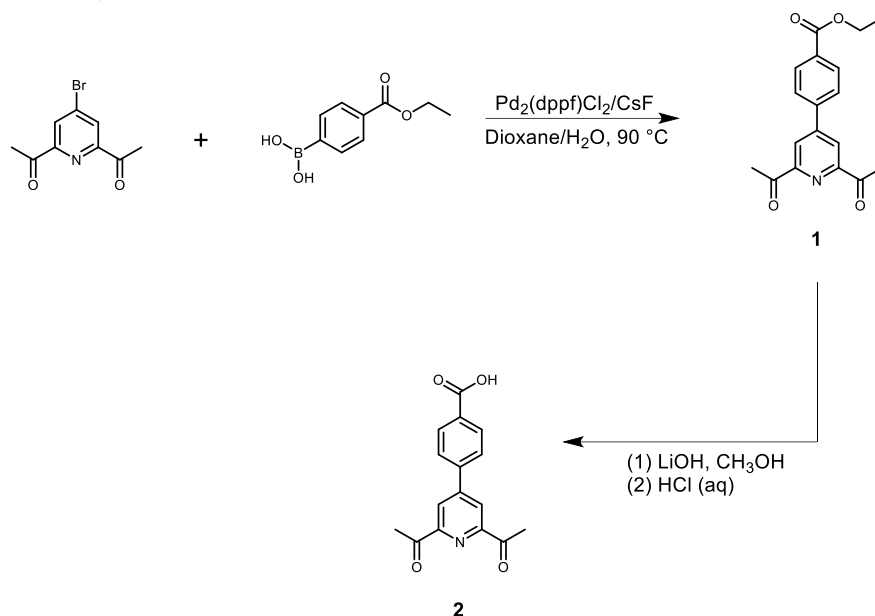
4-bromo-2,6-diacetylpyridine was synthesized through a reported method.¹ Other materials and solvents were purchased and directly used without further purification.

Nuclear magnetic resonance (NMR) spectra were recorded on Bruker spectrometers (Avance III 600: ¹H 600 MHz, ¹³C 151 MHz; Avance III 400: ¹H 400 MHz) at 298 K. ¹H NMR spectra are referred to the TMS signal and ¹³C NMR spectra are referred to the residual solvent signal. Data for ¹H NMR are reported as follows: chemical shifts (δ ppm), multiplicities (s = singlet, d = doublet, t = triplet, q = quartet, m = multiplet, br = broad). Coupling constants (J) were reported in Hz. High resolution electrospray ionization mass spectrometry (HR-ESI) experiments were measured with a Waters Synapt G2-Si Ion Mobility-Q-TOF High Resolution LC-MS instrument. Digital photographs were obtained by a Nikon Y-TV55 camera. Thermogravimetric analysis was carried out on a NETZSCH TG209 system under N₂ atmosphere in the range of 30-800 °C at a heating rate of 10 °C min⁻¹. Bruker D8 VENTURE PHOTON II MetalJet. Powder X-ray diffraction measurement was recorded on a Bruker D8 powder X-ray diffractometer with Cu-K α radiation ($\lambda = 1.5406 \text{ \AA}$). Scanning Electron Microscopy images were recorded using a SU8010 ultra-high resolution field emission scanning electron microscope. Elemental distribution was examined by Thermal Field Emission Environmental energy dispersive spectroscopy (Quanta 400F).

Single-Crystal X-ray Crystallography: The Single-Crystal X-ray diffraction data were collected on a SuperNova AtlasS2 diffractometer using Cu radiation ($\lambda = 1.54184$) at 150 K. Using Olex2,² the structure was solved with the Intrinsic Phasing structure solution program and refined with the ShelXL refinement package. The unit cell contains highly disordered solvent molecules including pyridine and N, N-dimethylformamide, which could not be modelled satisfyingly. These disordered solvent molecules and free H₂O were removed using the solvent masking procedure in Olex2,³ and thus 474 electrons were removed from the unit-cell. The contents of the solvent are not represented in the unit cell contents in the crystal data. Crystallographic data for **S-CM-1** are summarized in **Table S1**.

2. Synthesis

Scheme S1. The synthetic route of **1** and **2**.



1: In a 50 mL two-necked flask, a mixture of 4-Bromo-2,6-diacetylpyridine (2 mmol, 482 mg), 4-dihydroxyboranyl-benzoic acid ethyl ester (3 mmol, 582 mg), $\text{Pd}_2(\text{dppf})\text{Cl}_2$ (0.01 mmol, 73.1 mg), and CsF (10 mmol, 1.5 g) in 20 mL of Dioxane/ H_2O (4:1) was degassed under freeze-pump-thaw for three cycles and reacted at $90\text{ }^\circ\text{C}$ for 48 hours. After cooling to room temperature, the solvent was removed under reduced pressure, and the resulting residue was extracted with dichloromethane ($15\text{ mL} \times 3$). Next, the collected solution was dried with anhydrous Na_2SO_4 . After filtering, the solvent was removed under reduced pressure. Finally, the resulting crude product was further purified on silica gel, utilizing petroleum ether/ethyl acetate (5:1) as the eluent, resulting in the isolation of **1** as a white solid with a yield of 80% (497.6 mg). **MS m/z:** $[\text{M}+\text{Na}]^+$ calculated for $\text{C}_{18}\text{H}_{17}\text{NO}_4\text{Na}$: 334.10, found: 334.58. ^1H NMR (600 MHz, Chloroform-*d*) δ 8.50 (s, 2H), 8.21 (d, $J = 8.0\text{ Hz}$, 2H), 7.83 (d, $J = 8.1\text{ Hz}$, 2H), 4.45 (q, $J = 7.1\text{ Hz}$, 2H), 2.86 (s, 6H), 1.46 (t, $J = 7.1\text{ Hz}$, 3H). ^{13}C NMR (101 MHz, CDCl_3) δ 199.47, 166.01, 153.64, 149.62, 140.97, 131.80, 130.60, 127.26, 122.54, 61.44, 25.83, 14.44.

20230316_230316145228 #727-760 RT: 1.73-1.85 AV: 54 SB: 398 0.58-1.01, 1.07-1.57 NL: 1.15E6
T: ITMS + c ESI/Fulms [100.00-1000.00]

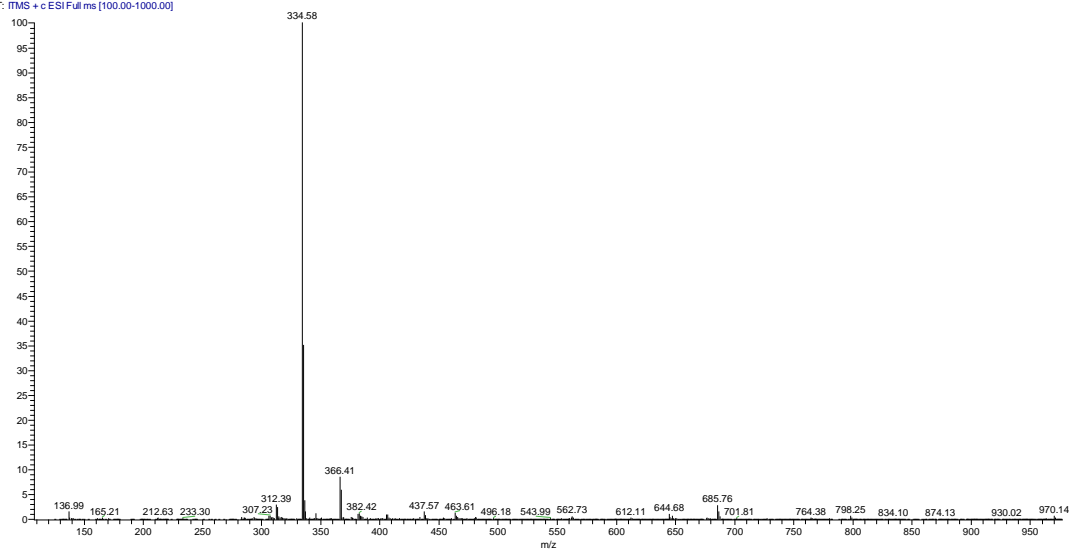


Figure S1. low-resolution MS spectrum of **1**.

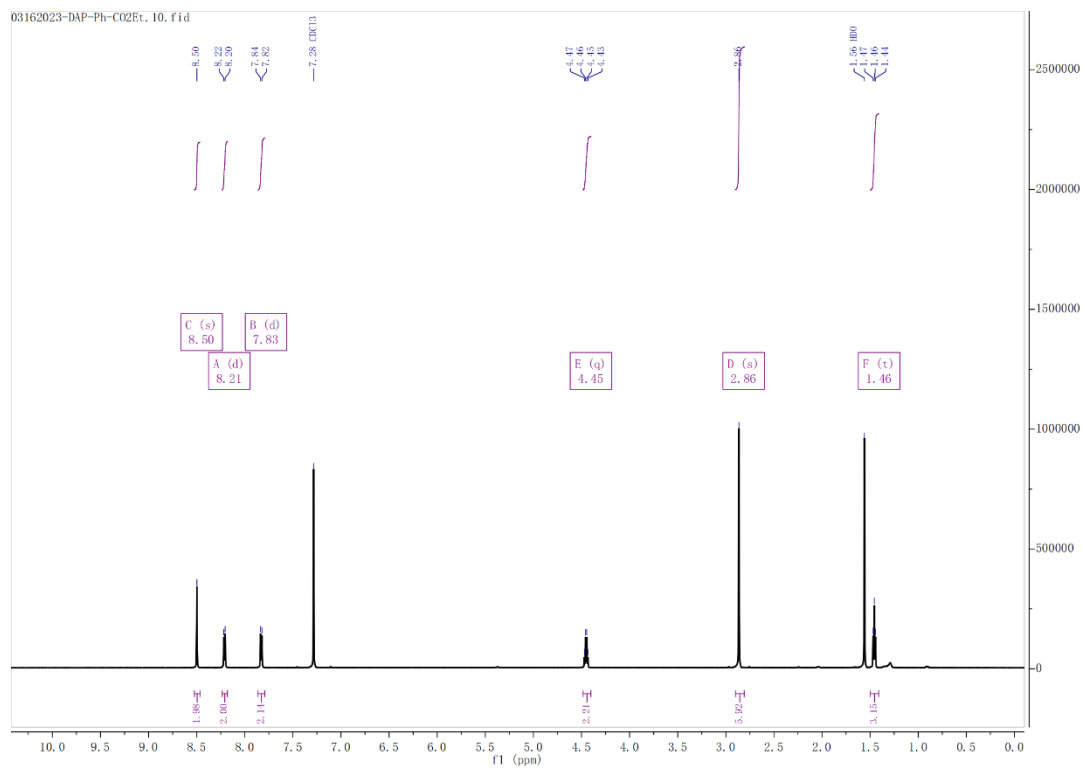


Figure S2. ¹H NMR spectrum of **1** (CDCl₃, 600 MHz).

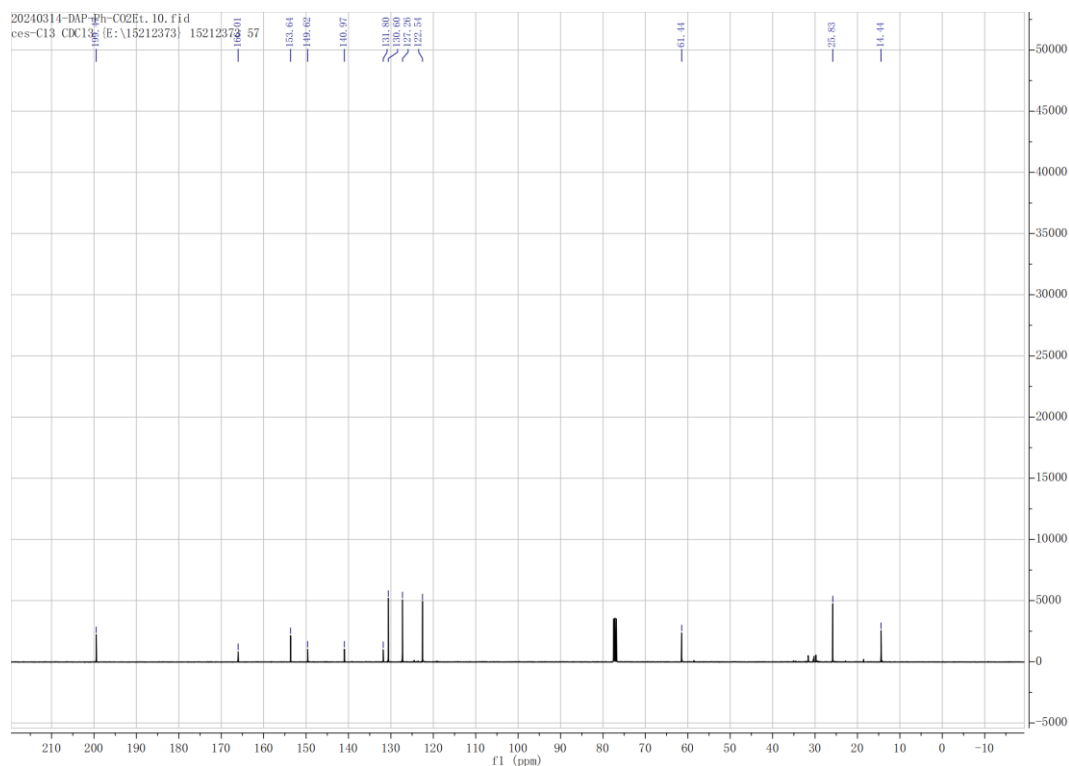


Figure S3. ^{13}C NMR spectrum of **1** (CDCl_3 , 101 MHz).

2: To a 50 mL flask, compound **1** (1 mmol, 311.0 mg) and LiOH (1.2 mmol, 28.8 mg) were dissolved in 10 mL CH_3OH , and the mixture was refluxed for 5 h. After cooling to room temperature, the solvent was removed under reduced pressure, and the resulting residue was extracted with ethyl acetate for three times (10 mL \times 3). Next, the collected solution was dried with anhydrous Na_2SO_4 . Following filtration, pure compound **2** with a nearly quantifiable yield was obtained by rotary evaporation at reduced pressure. **MS m/z:** $[\text{M}+\text{Na}]^+$ calculated for $\text{C}_{16}\text{H}_{13}\text{NO}_4\text{Na}$: 306.07, found: 306.15. ^1H NMR (400 MHz, DMSO-d_6) δ 8.45 (s, 2H), 8.14-8.01 (m, 4H), 2.78 (s, 6H).

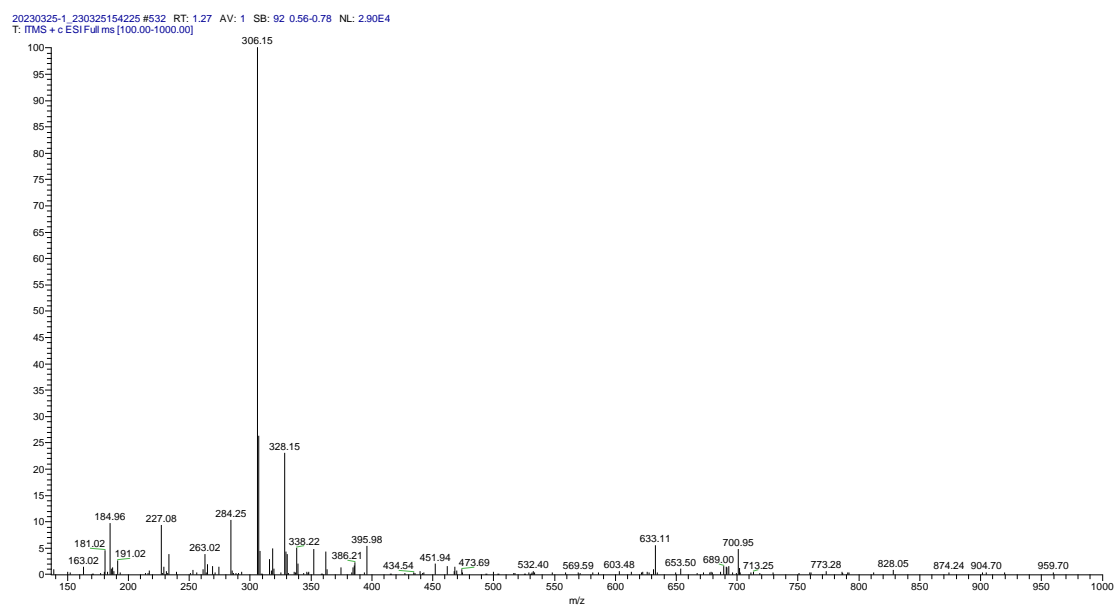


Figure S4. low-resolution MS spectrum of **2**.

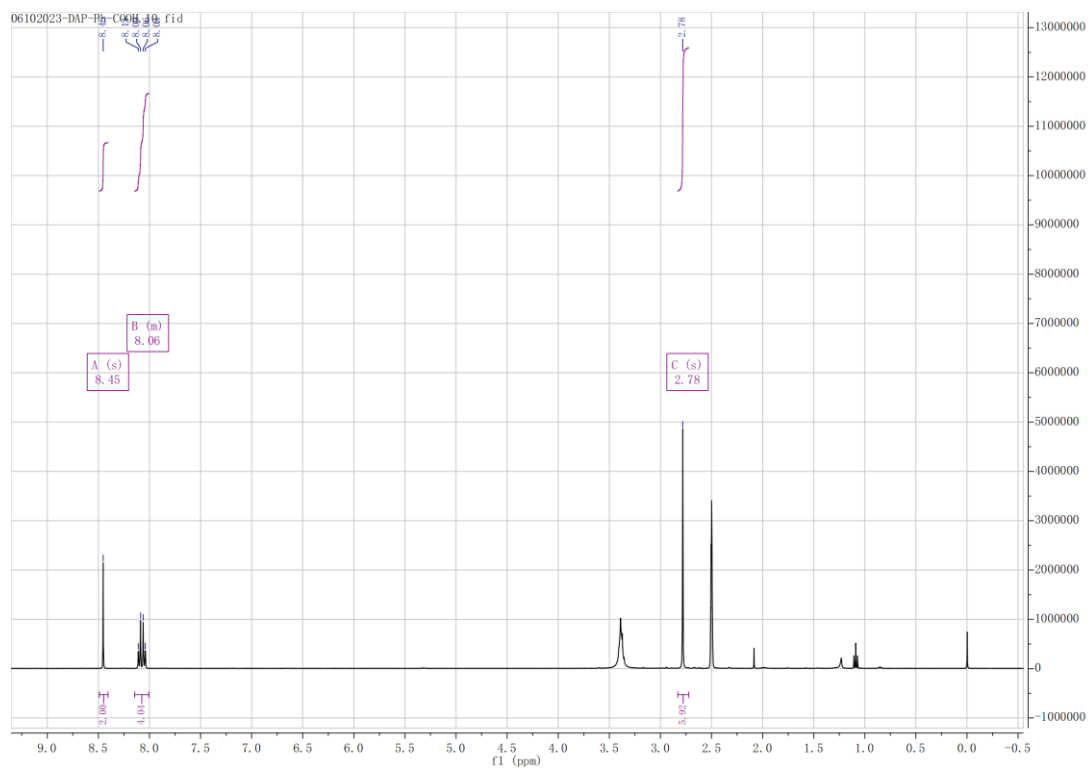
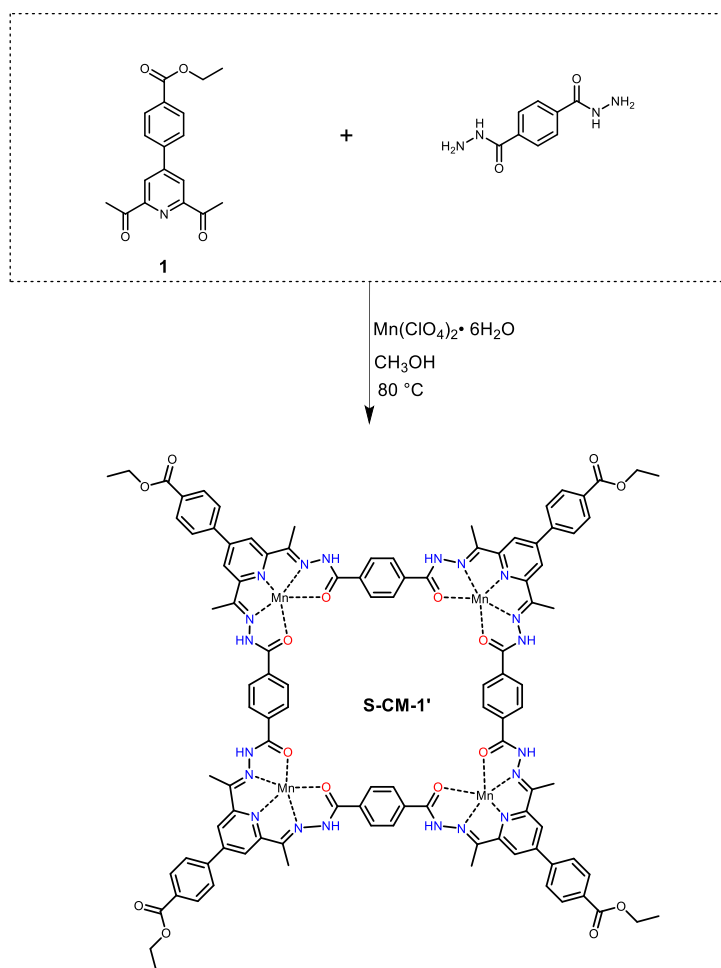


Figure S5. ¹H NMR spectrum of **2** (DMSO-d₆, 400 MHz).

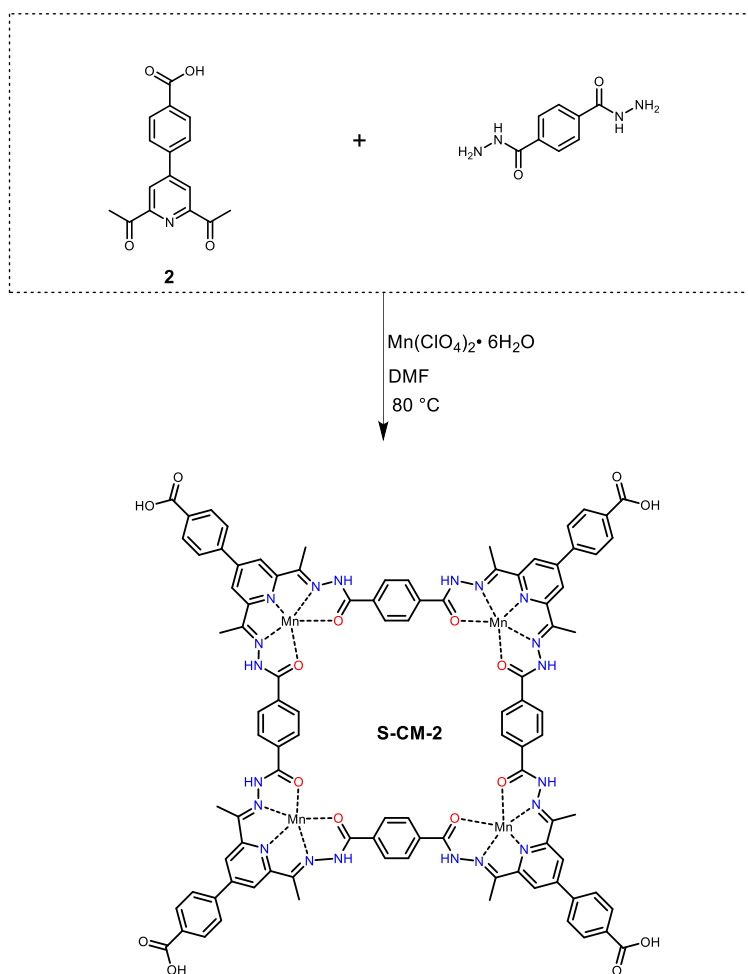
Scheme S2. Synthetic route of **S-CM-1'**.



S-CM-1': To a 100 mL flask, compound **1** (0.5 mmol, 155.5 mg), terephthalic dihydrazide (0.5 mmol, 97 mg), $\text{Mn}(\text{ClO}_4)_2 \cdot 6\text{H}_2\text{O}$ (0.5 mmol, 183 mg) and CH_3OH (50 mL) were added. Next, the mixture was refluxed at $85\text{ }^\circ\text{C}$ for 12 hours. Upon cooling to room temperature, the solvent was removed under reduced pressure, resulting in a yellow product of **S-CM-1'** with a quantitative yield.

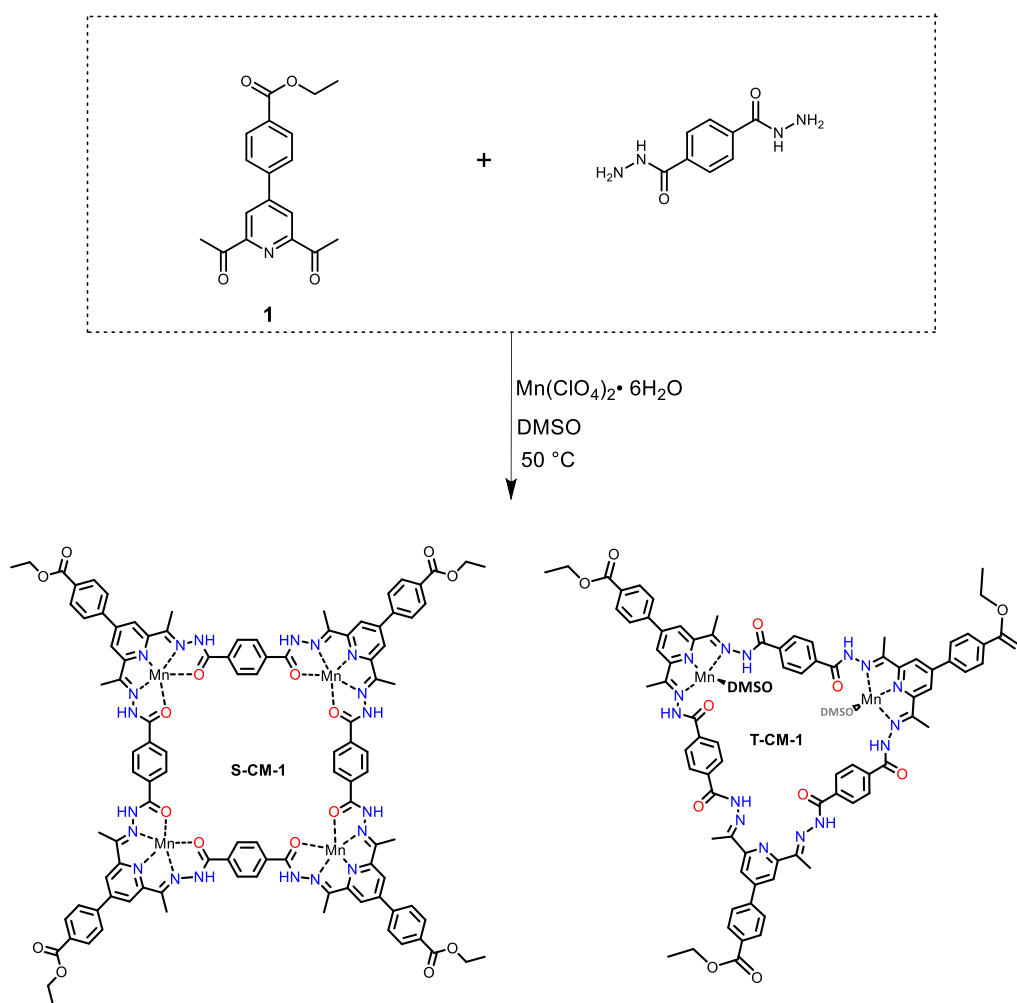
S-CM-1: First, 50 mg of **S-CM-1'** was dissolved in 3 mL DMF in a 5 mL vial. Following, pyridine was slowly diffused into the solution to obtain single crystals for single crystal X-ray diffraction. The resulting crystals were collected via centrifugation, washed with ethyl ether, and air dried at room temperature.

Scheme S3. Synthesis of **S-CM-2** in DMF.



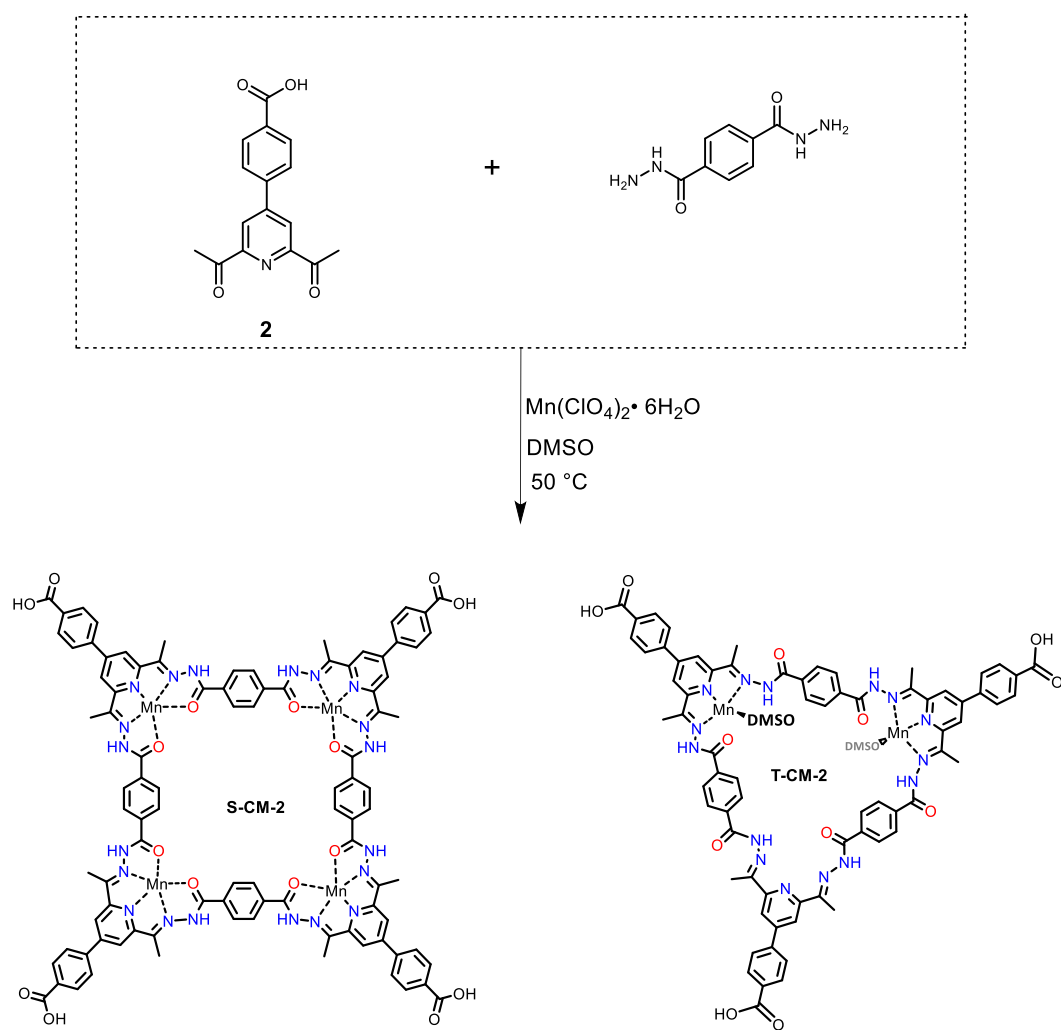
S-CM-2: To a 50 mL flask, compound **2** (0.1 mmol, 28.3 mg), terephthalic dihydrazide (0.1 mmol, 19.4 mg), $\text{Mn}(\text{ClO}_4)_2 \cdot 6\text{H}_2\text{O}$ (0.1 mmol, 36.6 mg) and DMF (10 mL) were added. Next, the mixture was reacted at $85\text{ }^\circ\text{C}$ for 12 hours. After cooling to room temperature, the solution was poured into 50 mL of ethyl ether, which resulted in the formation of a yellow product in an almost quantitative yield.

Scheme S4. Synthesis of the **S-CM-1** and **T-CM-1** mixture in DMSO.



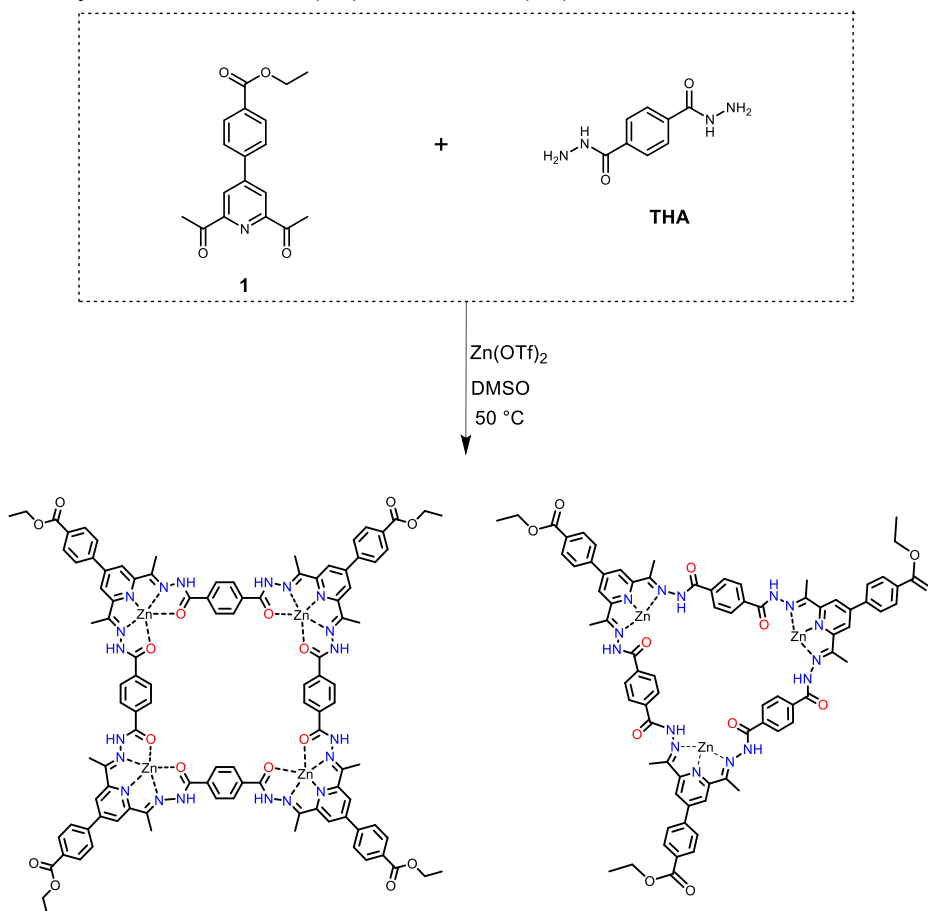
Mixture of **S-CM-1** and **T-CM-1**: to a 20 mL flask, ligand **1** (0.1 mmol, 31.1 mg), terephthalic dihydrazide (0.1 mmol, 19.4 mg), $\text{Mn}(\text{ClO}_4)_2 \cdot 6\text{H}_2\text{O}$ (0.1 mmol, 36.6 mg) and DMSO (5 mL) were charged. Next, the mixture was reacted at 50°C for 12 hours. Without any treatment, the reaction solution was directly used for high-resolution mass spectrometry.

Scheme S5. Synthesis of **S-CM-2** and **T-CM-2** mixture in DMSO.



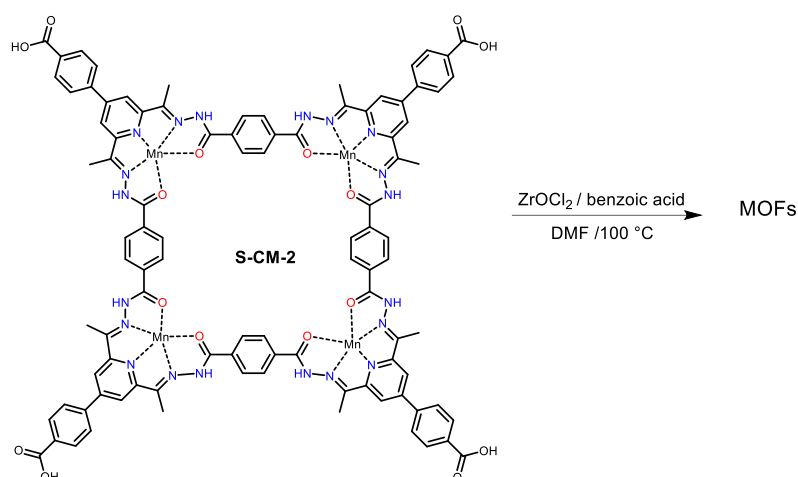
Mixture of **S-CM-2** and **T-CM-2**: to a 20 mL flask, ligand **2** (0.1 mmol, 28.3 mg), terephthalic dihydrazide (0.1 mmol, 19.4 mg), $\text{Mn}(\text{ClO}_4)_2 \cdot 6\text{H}_2\text{O}$ (0.1 mmol, 36.6 mg) and DMSO (5 mL) were charged. Next, the mixture was reacted at 50 °C for 12 hours. Without any treatment, the reaction solution was directly used for high-resolution mass spectrometry.

Scheme S6. Synthesis of **S-CM-1 (Zn)** and **T-CM-1 (Zn)** mixture in DMSO.



Mixture of **S-CM-1 (Zn)** and **T-CM-1 (Zn)**: to a 20 mL flask, ligand **1** (0.1 mmol, 31.1 mg), terephthalic dihydrazide (0.1 mmol, 19.4 mg), Zn (0.1 mmol, 36.3 mg) and DMSO (5 mL) were charged. Next, the mixture was reacted at $50\text{ }^\circ\text{C}$ for 12 hours. Without any treatment, the reaction solution was directly used for high-resolution mass spectrometry.

Scheme S7. Synthesis of the zirconium-based MOFs.



Solution a: to a 50 mL flask, ligand **2** (0.05 mmol, 14.2 mg), terephthalic dihydrazide (0.05 mmol, 9.7 mg), $\text{Mn}(\text{ClO}_4)_2 \cdot 6\text{H}_2\text{O}$ (0.05 mmol, 18.3 mg) and 10 mL of DMF were added, and the mixture was reacted at $80\text{ }^\circ\text{C}$ for 12 hours. The resulting solution containing **S-CM-2** was cooled to room temperature and stored for the next step.

Solution b: 20 mg of ZrOCl_2 and 1 g of benzoic acid were dissolved in 2 mL of DMF in a 20 mL vial. After ultrasound for 5 minutes, the vial was transferred to an oven at $100\text{ }^\circ\text{C}$ for 1 hour. Finally, leave the vial cool to room temperature prior to use.

Synthesis of the zirconium-based MOFs: Solutions **a** and **b** were combined in a 20 mL vial. Subsequently, the vial was placed in an oven preheated to $100\text{ }^\circ\text{C}$ for 12 hours, yielding a brown-yellow product. After centrifugation, the obtained solids were washed with DMF for 3 times, ethanol for 3 times, and finally dried under vacuum at $80\text{ }^\circ\text{C}$ for 24 hours (50% yield based on the metal source).

3. High-resolution MS analysis

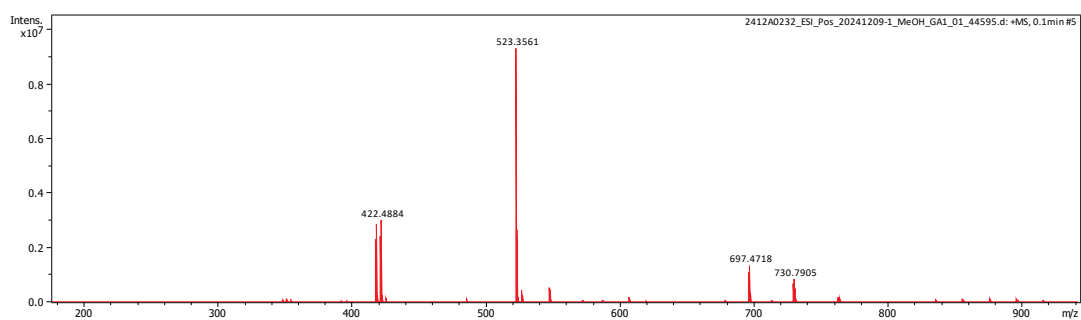


Figure S6. HR-MS spectra of S-CM-1'.

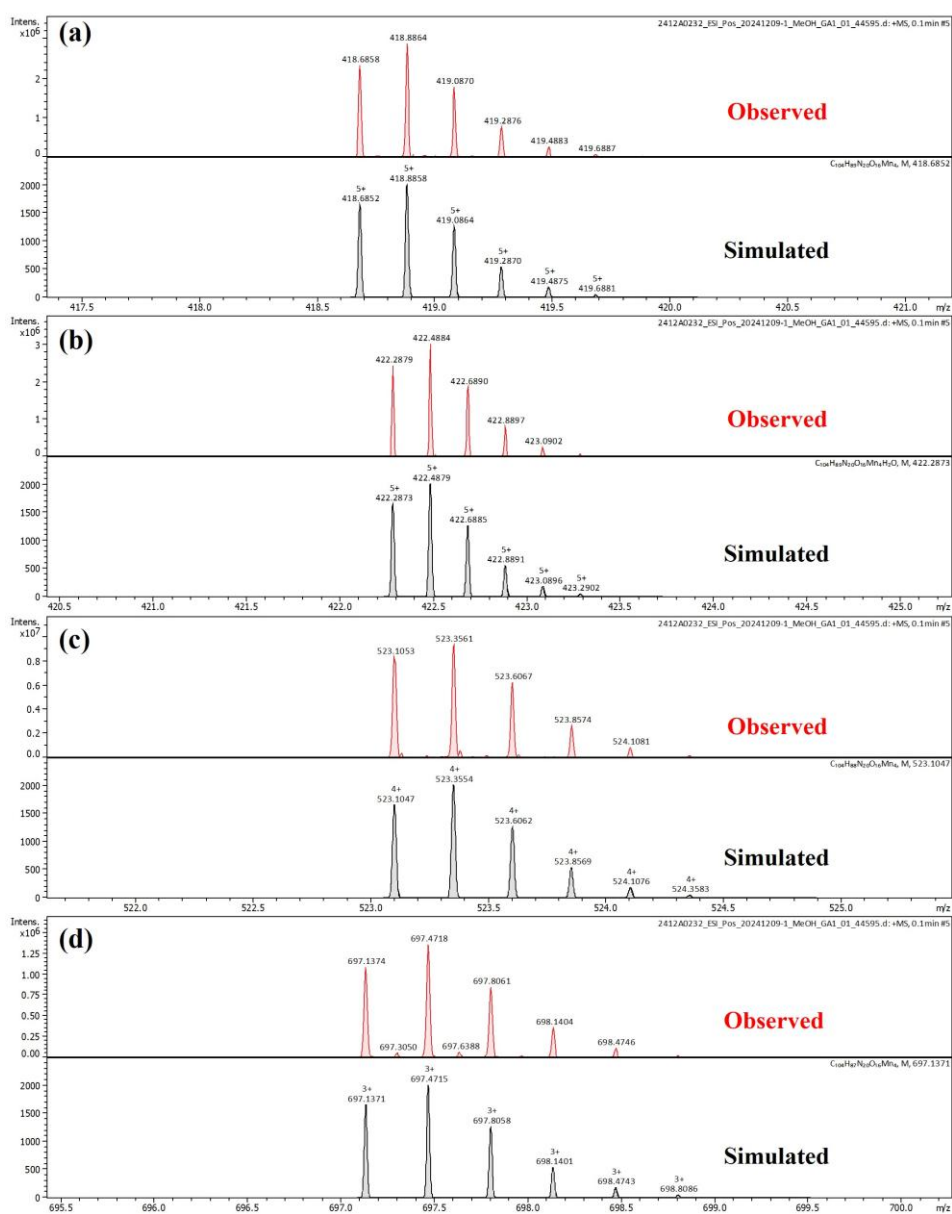


Figure S7. The observed and simulated MS peaks of S-CM-1'. (a) $[C_{104}H_{89}N_{20}O_{16}Mn_4]^{5+}$, (b) $[C_{104}H_{89}N_{20}O_{16}Mn_4(H_2O)]^{5+}$, (c) $[C_{104}H_{88}N_{20}O_{16}Mn_4]^{4+}$, (d) $[C_{104}H_{87}N_{20}O_{16}Mn_4]^{3+}$.

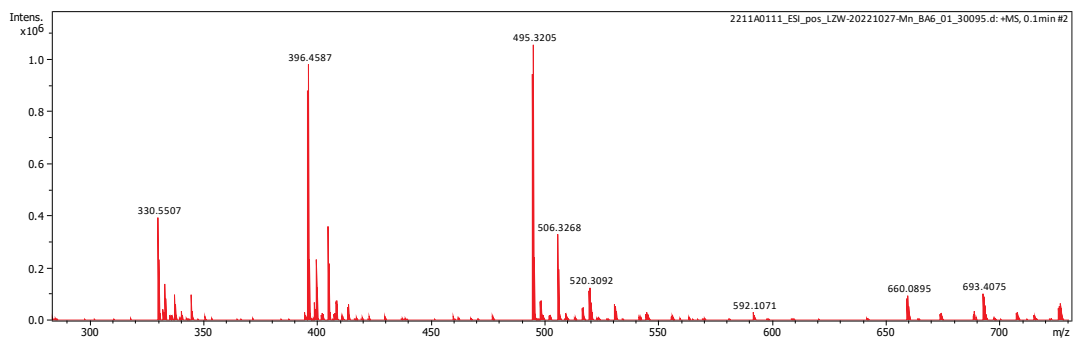


Figure S8. HR-MS spectra of S-CM-2.

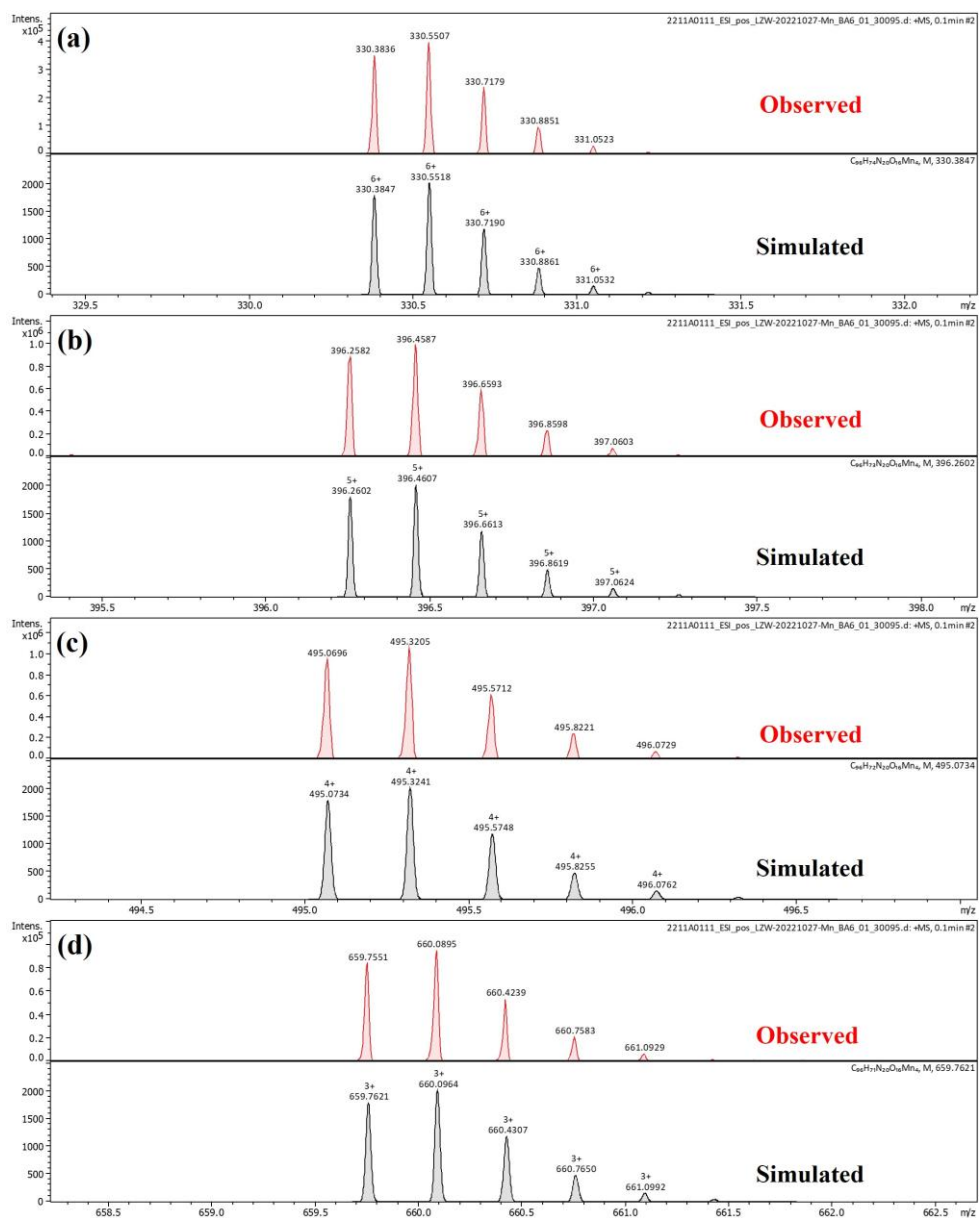


Figure S9. The observed and simulated MS peaks of S-CM-2. (a) $[C_{96}H_{74}N_{20}O_{16}Mn_4]^{6+}$, (b) $[C_{96}H_{73}N_{20}O_{16}Mn_4]^{5+}$, (c) $[C_{96}H_{72}N_{20}O_{16}Mn_4]^{4+}$, (d) $[C_{96}H_{71}N_{20}O_{16}Mn_4]^{3+}$.

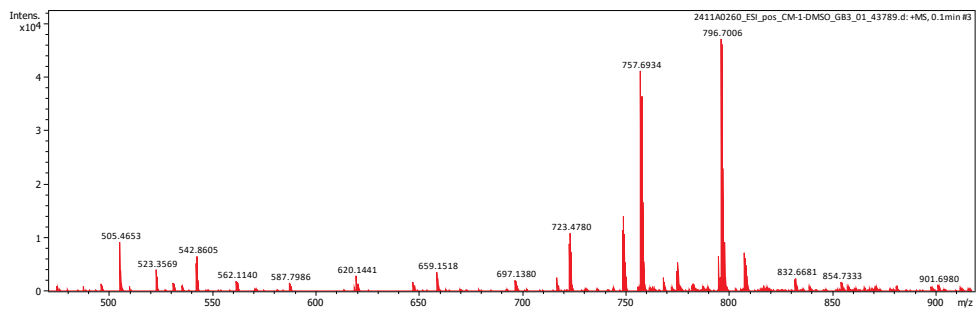


Figure S10. HR-MS spectra of the S-CM-1 and T-CM-1 mixture.

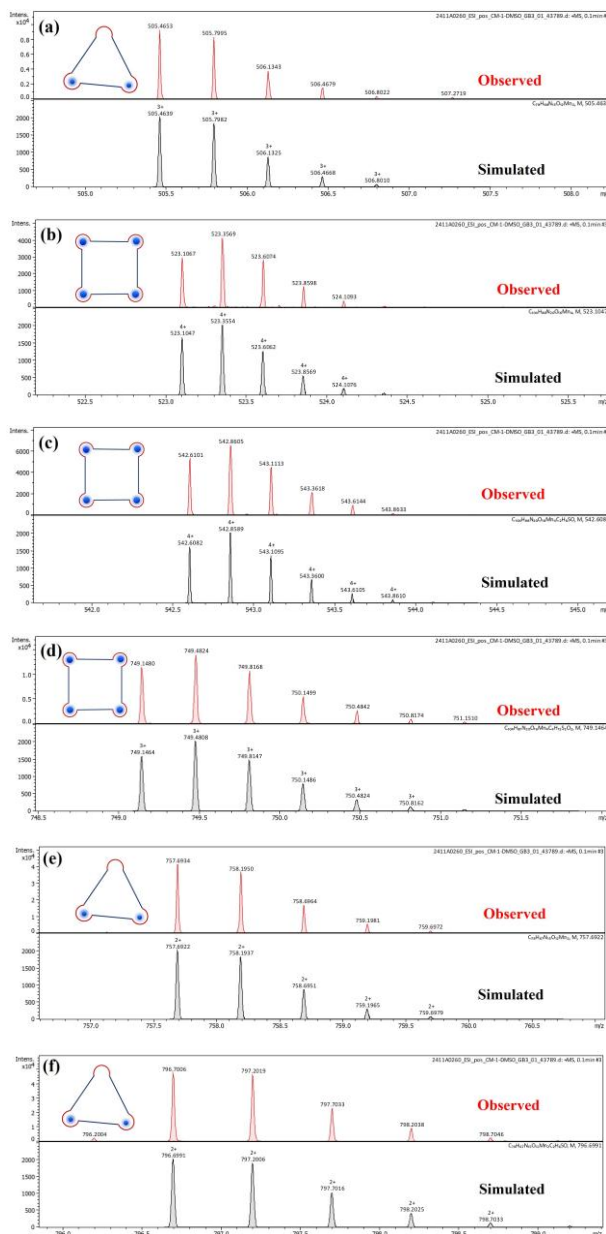


Figure S11. The observed and simulated MS peaks of the S-CM-1 and T-CM-1 mixtures. (a) $[C_{78}H_{68}N_{15}O_{12}Mn_2]^{3+}$, (b) $[C_{104}H_{88}N_{20}O_{16}Mn_4]^{4+}$, (c) $[C_{104}H_{88}N_{20}O_{16}Mn_4(DMSO)]^{4+}$, (d) $[C_{104}H_{87}N_{20}O_{16}Mn_4(DMSO)_2]^{3+}$, (e) $[C_{78}H_{67}N_{15}O_{12}Mn_2]^{2+}$, (f) $[C_{78}H_{67}N_{15}O_{12}Mn_2(DMSO)]^{2+}$.

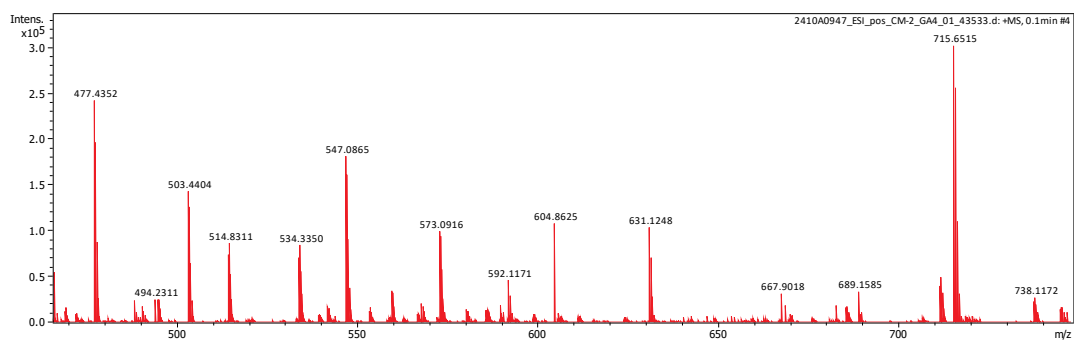


Figure S12. HR-MS spectra of the S-CM-2 and T-CM-2 mixtures.

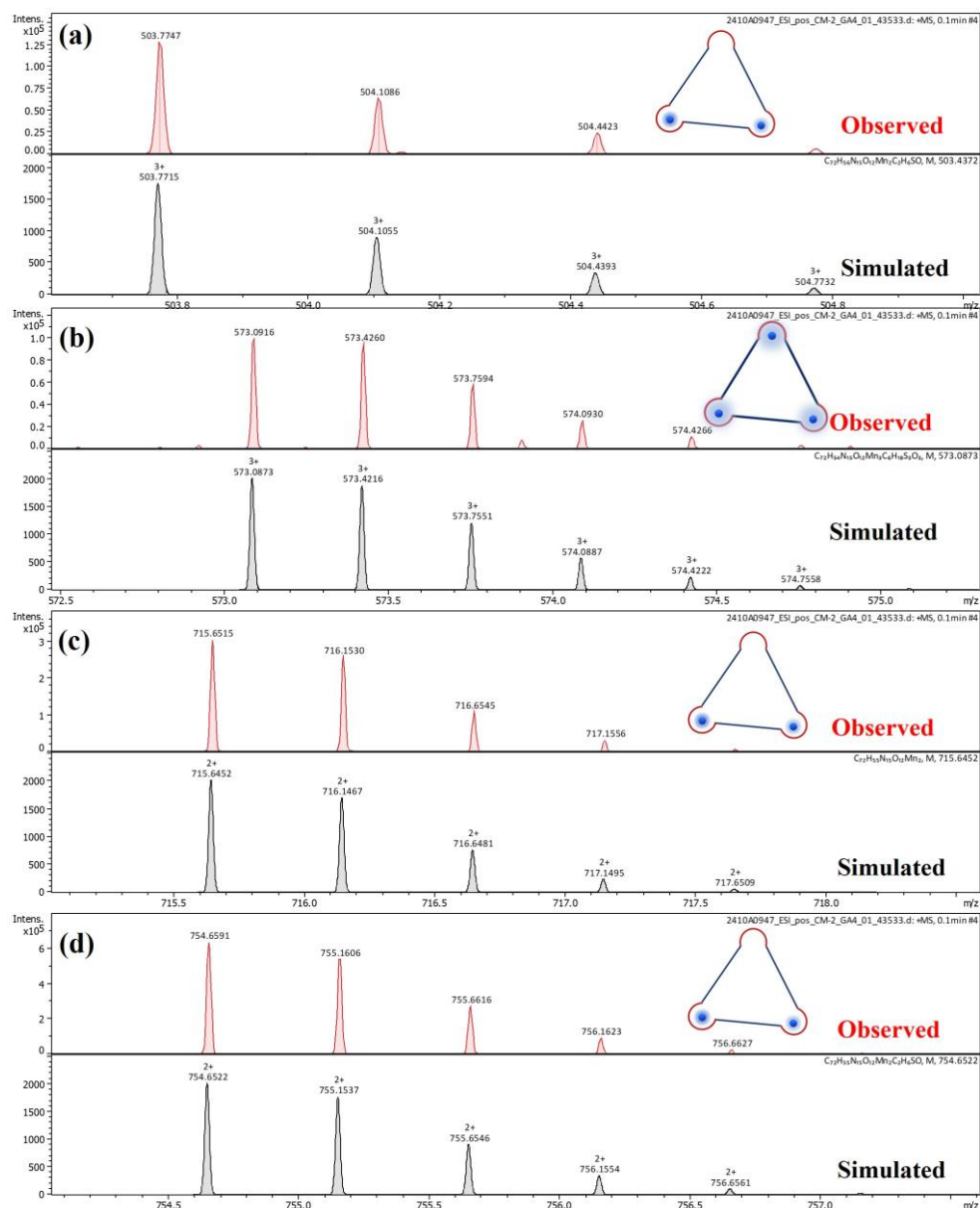


Figure S13. The observed and simulated MS peaks of the S-CM-2 and T-CM-2 mixtures. (a) $[C_{72}H_{56}N_{15}O_{12}Mn_2(DMSO)]^{3+}$, (b) $[C_{72}H_{54}N_{15}O_{12}Mn_3(DMSO)_3]^{3+}$, (c) $[C_{72}H_{55}N_{15}O_{12}Mn_2]^{2+}$, (d) $[C_{72}H_{55}N_{15}O_{12}Mn_2(DMSO)]^{2+}$.

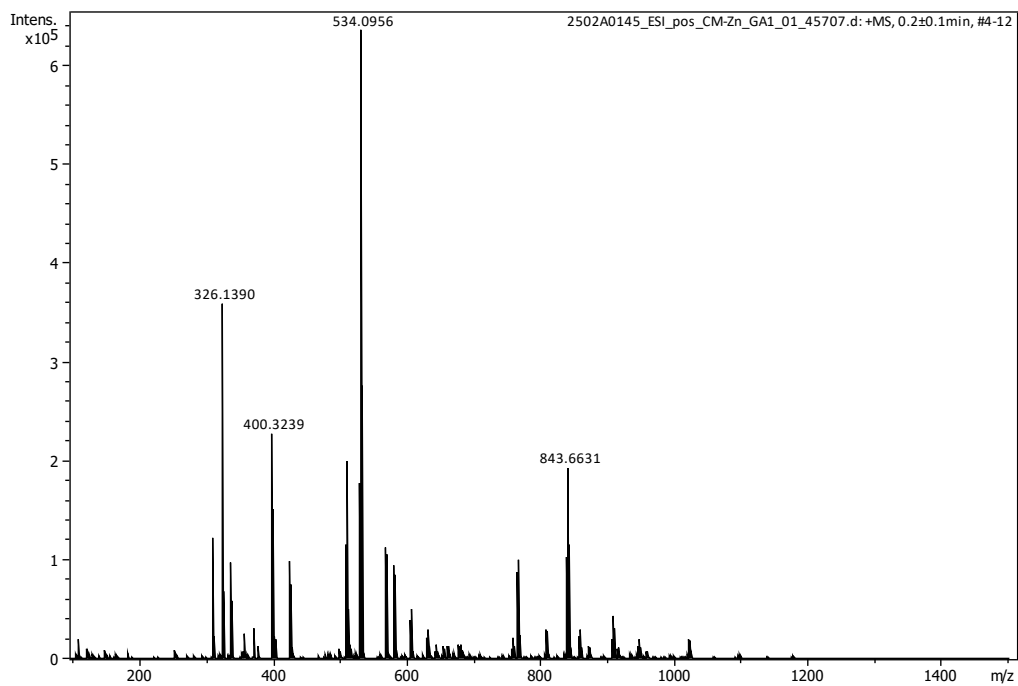


Figure S14. HR-MS spectra of the S-CM-1 (Zn) and T-CM-1 (Zn) mixtures.

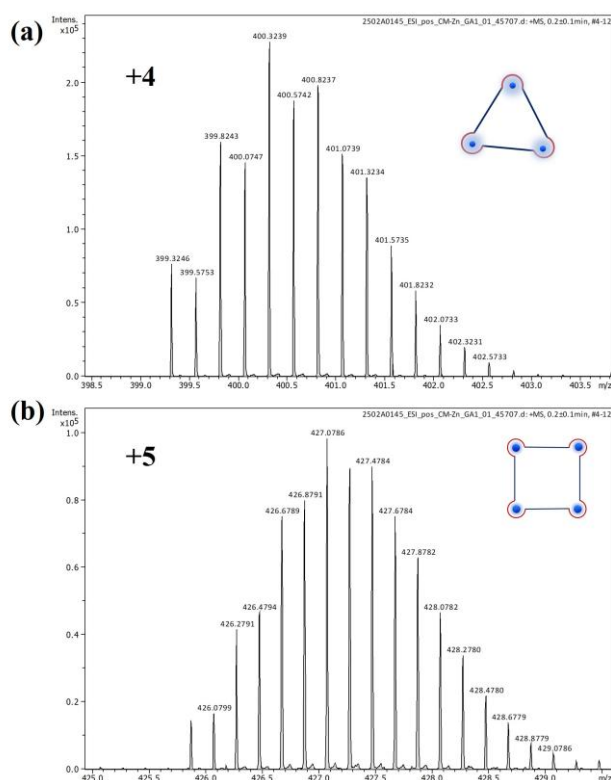


Figure S15. The observed MS peaks of the (a) T-CM-1 (Zn), $[C_{78}H_{67}N_{15}O_{12}Mn_3]^{4+}$; (b) S-CM-1 (Zn), $[C_{104}H_{89}N_{20}O_{16}Zn_4]^{5+}$.

4. Single-crystal X-ray analysis.

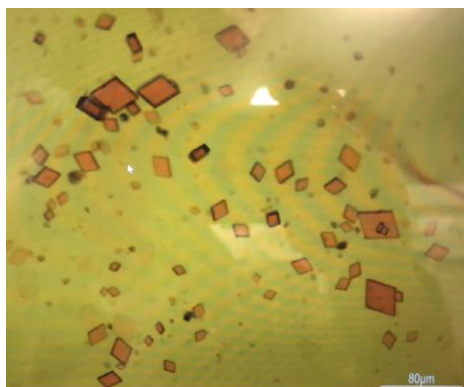


Figure S16. Digital photograph of S-CM-1 single crystals.

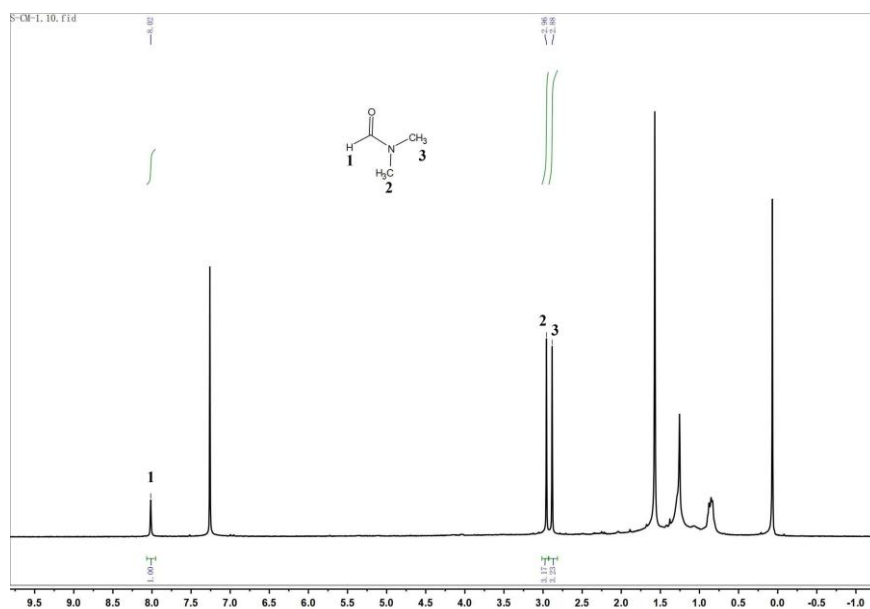


Figure S17. ¹H NMR spectra of the solvent molecules extracted from the S-CM-1 crystals. The S-CM-1 crystals were immersed in CDCl₃ for 1 hour, and the filtrated clear liquid was used for ¹H NMR experiment. The peaks at 2.88, 2.96, and 8.02 ppm are attributed to DMF, confirming the presence of DMF in the S-CM-1 crystals.

Table S1. Crystallographic data of **S-CM-1**.

Name	S-CM-1
CCDC number	2415029
Empirical formula	C ₁₄₄ H ₁₂₄ Mn ₄ N ₂₈ O ₁₆
Formula weight	2722.46
Temperature/K	150.15
Crystal system	triclinic
Space group	<i>P</i> -1
<i>a</i> /Å	9.1397(10)
<i>b</i> /Å	19.8181(19)
<i>c</i> /Å	26.775(3)
α /°	88.264(8)
β /°	88.730(8)
γ /°	78.204(9)
Volume/Å ³	4744.6(9)
<i>Z</i>	1
ρ_{calc} g/cm ³	0.953
μ /mm ⁻¹	2.553
<i>F</i> (000)	1412.0
Radiation/Å	CuK α (λ = 1.54184)
2θ range for data collection/°	5.698 to 130.176
Index ranges	-10 $\leq h \leq$ 9, -23 $\leq k \leq$ 22, -31 $\leq l \leq$ 29
Reflections collected	32312
Independent reflections	16129 [R_{int} = 0.1436, R_{sigma} = 0.2254]
Data/restraints/parameters	16129/84/833
Goodness-of-fit on F^2	0.906
Final <i>R</i> indexes [$I \geq 2\sigma(I)$]	R_1 = 0.0897, wR_2 = 0.2212
Final <i>R</i> indexes [all data]	R_1 = 0.1742, wR_2 = 0.2821

$$R_1 = \frac{\sum ||F_o| - |F_c||}{\sum |F_o|}, wR_2 = \left[\frac{\sum w(F_o^2 - F_c^2)^2}{\sum w(F_o^2)^2} \right]^{1/2}$$

Table S2. Hydrogen Bonds for **S-CM-1**.

D-H-A	d(D-H)/Å	d(H-A)/Å	d(D-A)/Å	D-H-A/°
C62-H62-N4	0.95	2.66	3.285(9)	123.5
C67-H67-N9	0.95	2.56	3.198(8)	124.6
C71-H71-O8 ¹	0.95	2.61	3.197(10)	120.3
C72-H72-O8 ¹	0.95	2.55	3.186(9)	124.8
C57-H57-N4	0.95	2.55	3.198(9)	125.9
C53-H53-N1	0.95	2.67	3.456(8)	140.6

Symmetry code: ¹-1+X, -1+Y, +Z

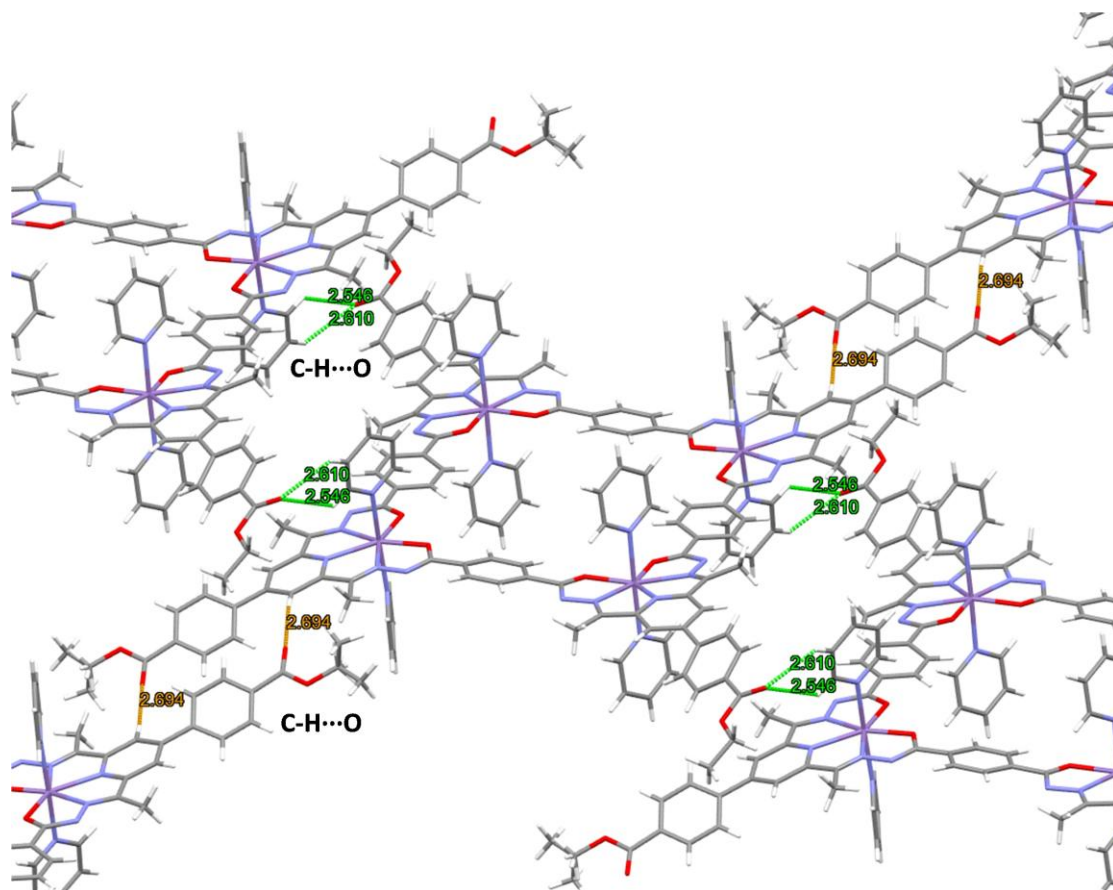


Figure S18. Hydrogen bonded network in **S-CM-1**. Each metallacycle forms multiple C-H...O interactions with the four adjacent metallacycles.

5. Hirshfeld surface analysis

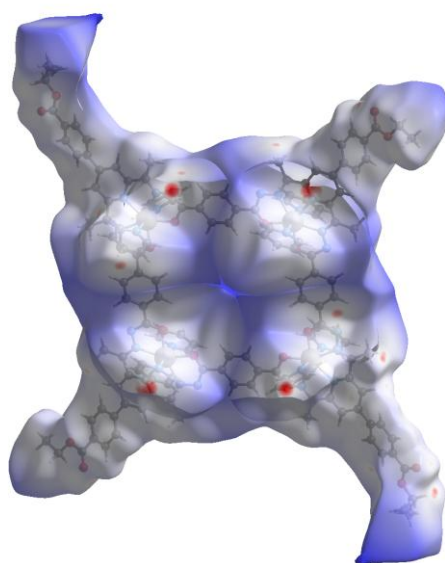


Figure S19. Hirshfeld surface of **S-CM-1** in the crystal structure.

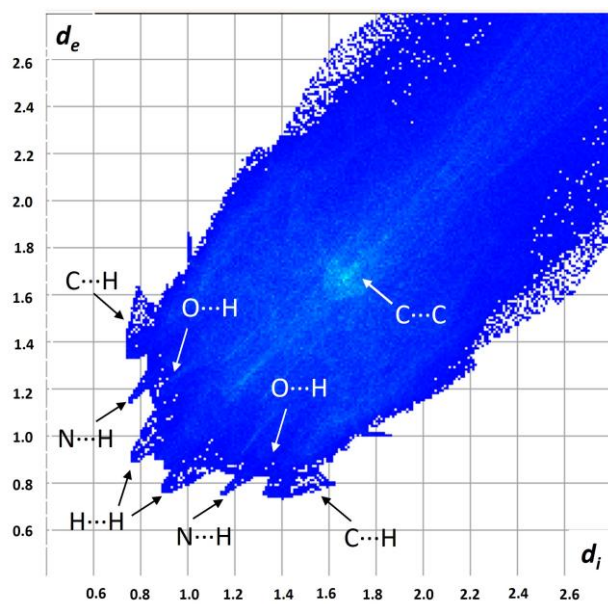


Figure S20. Fingerprint plots in crystal stacking found in S-CM-1.

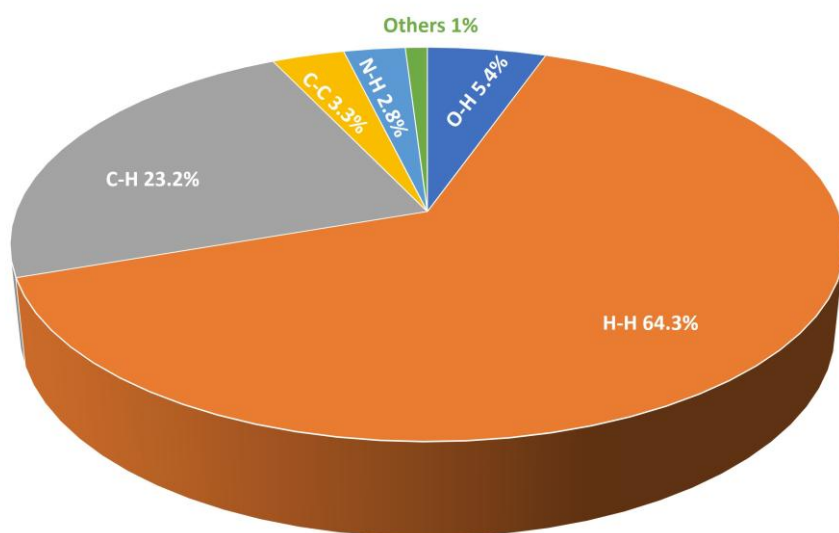


Figure S21. Individual atomic contact percentage contribution to the Hirshfeld surface.

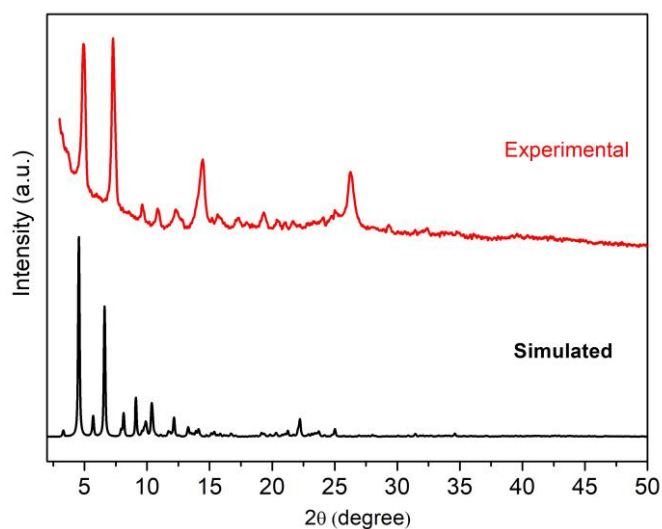


Figure S22. PXRD patterns of **S-CM-1**.

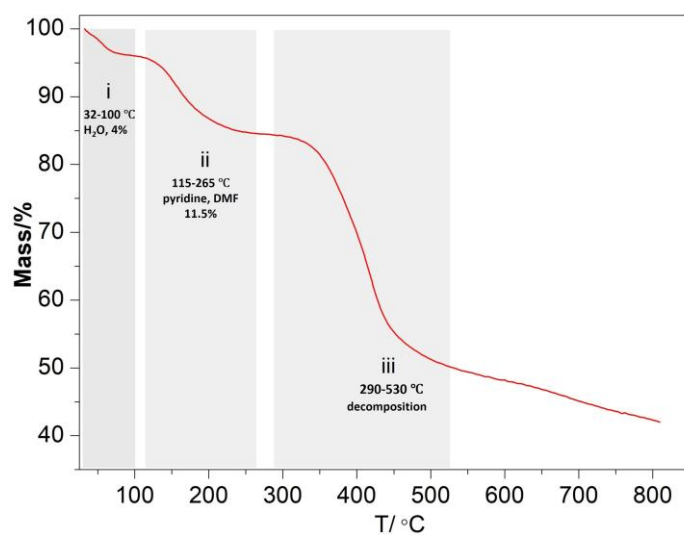


Figure S23. Thermogravimetric curve of **S-CM-1**. Three well-resolved weight loss regions are observed in the TG curves, which can be assigned to **(i)** the water physically absorbed in the crystals (32-100 °C, 4%); **(ii)** the uncoordinated, coordinated pyridine molecules, and DMF in the crystals (115-265 °C, 11.5%); and **(iii)** framework decomposition (290-530 °C).

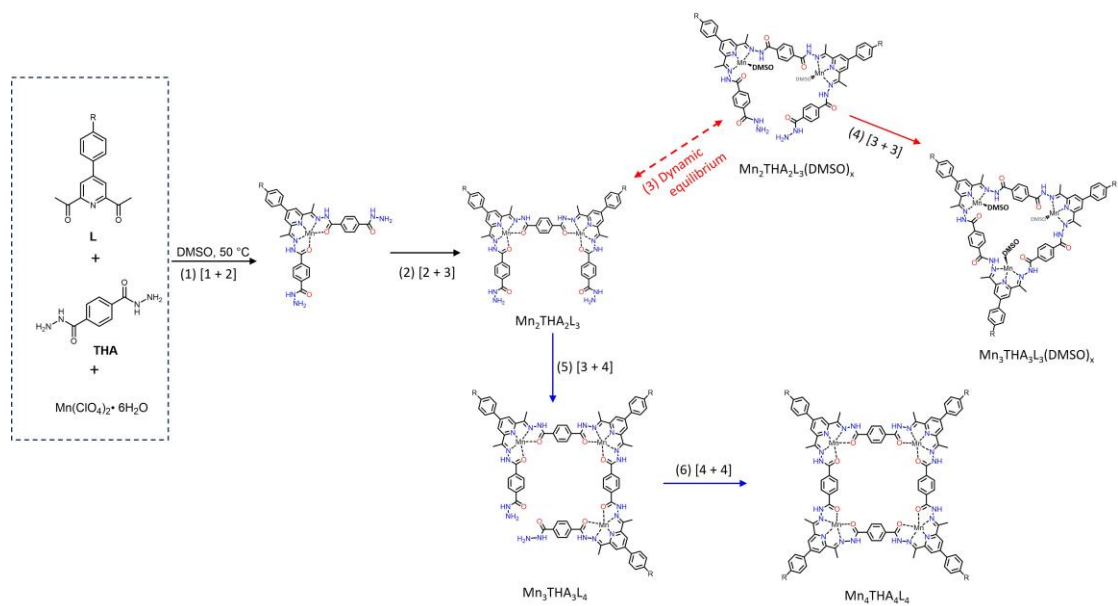
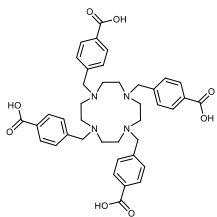
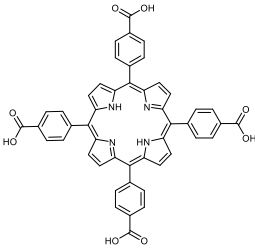
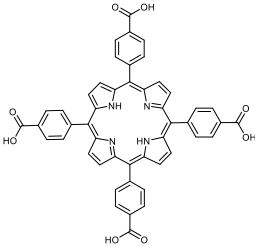
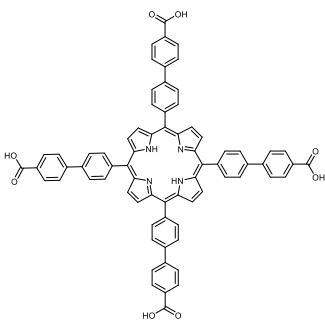
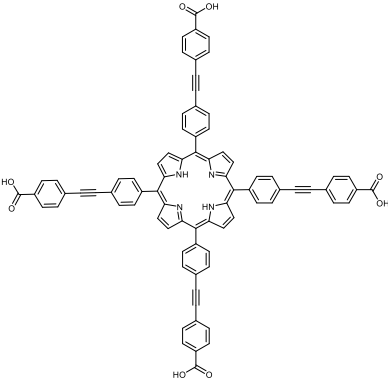


Figure S24. A plausible formation mechanism of the square and triangle mixtures.

6. Characterization of mMOF-1

Table S3. Summaries of typical Zr-based MOFs constructed from neutral C₄-symmetric ligands.

Name	Ligand	Connectivity	Topology	Reference
NU-1107		12-connect Zr ₆	<i>ftw</i>	4
PCN-222		8-connect Zr ₆	<i>csq</i>	5
PCN-224		6-connect Zr ₆	<i>she</i>	6
NU-1102		12-connect Zr ₆	<i>ftw</i>	7
NU-1104		12-connect Zr ₆	<i>ftw</i>	7

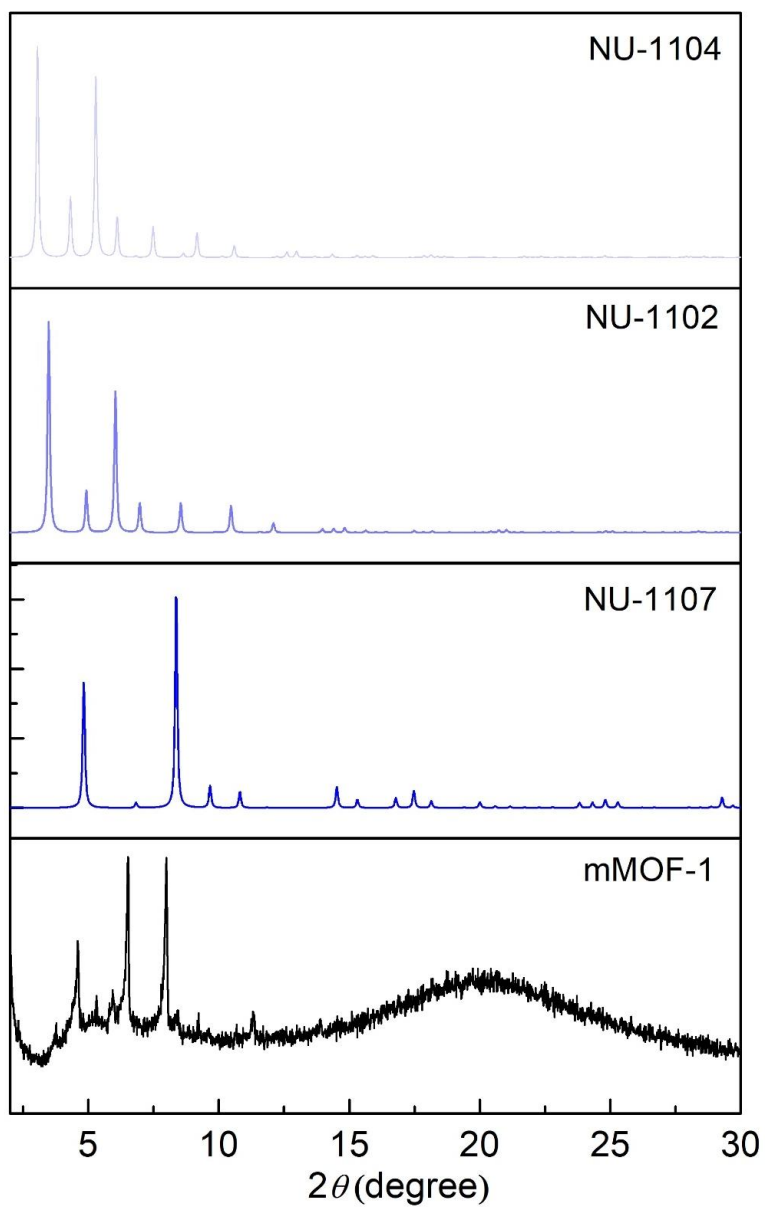


Figure S25. Comparisons of the PXRD patterns between **mMOF-1**, NU-1107, NU-1102, and NU-1104. All three typical MOFs are linked by 12-connect Zr_6 clusters and possess the *ftw* topology.

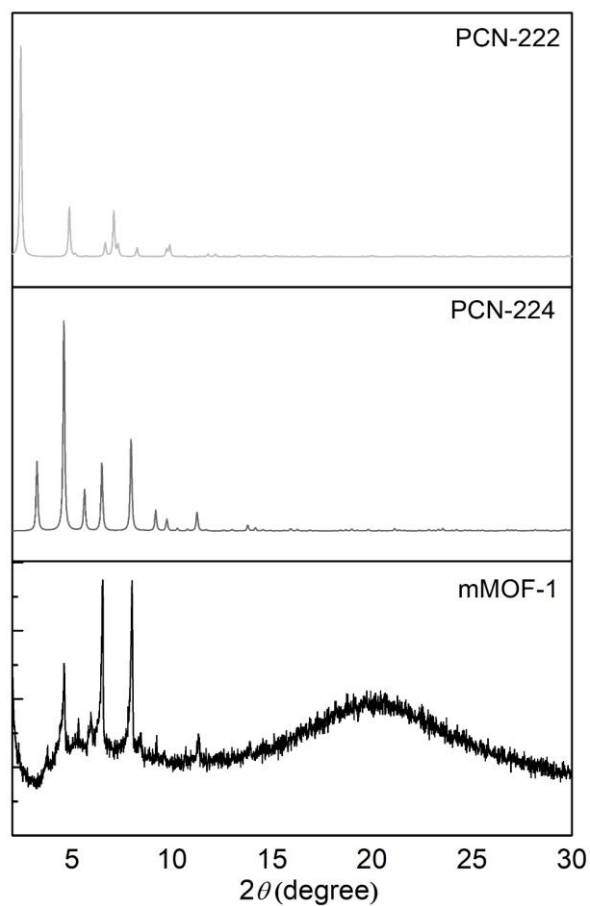


Figure S26. Comparisons of the PXRD patterns between **mMOF-1**, PCN-224, and PCN-222. PCN-222 is constructed from 8-connected Zr_6 clusters and exhibits a csq topology, whereas PCN-224 is linked by 6-connected Zr_6 clusters and features a she topology.

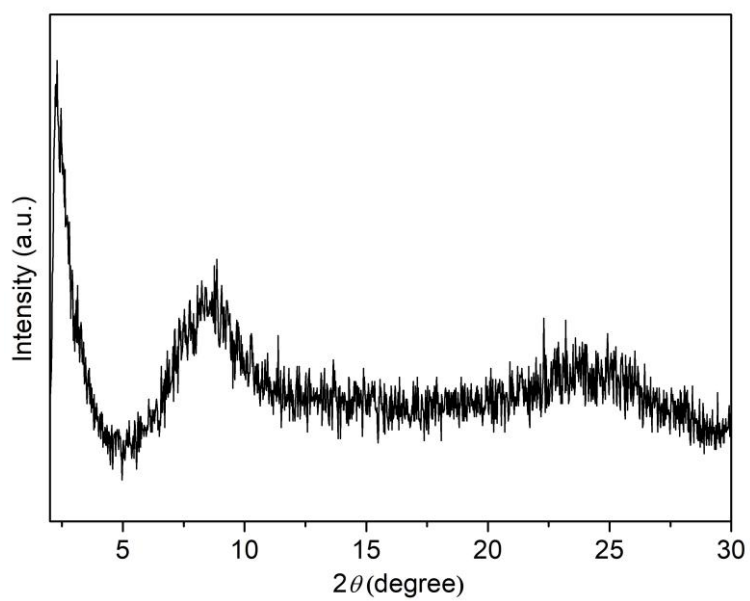


Figure S27. PXRD of mMOF-1 after drying.

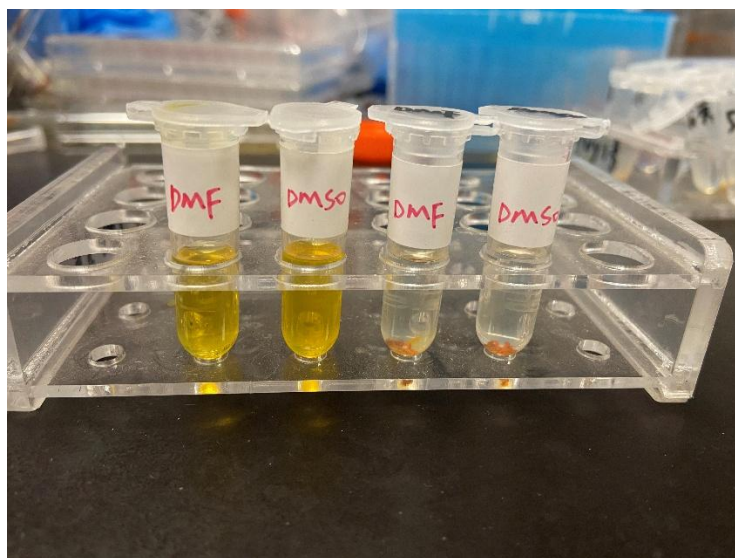


Figure S28. Solubility test of **S-CM-2** and **mMOF-1** in DMF and DMSO. **S-CM-2** is soluble in DMF and DMSO, whereas **mMOF-1** is insoluble in both solvents.

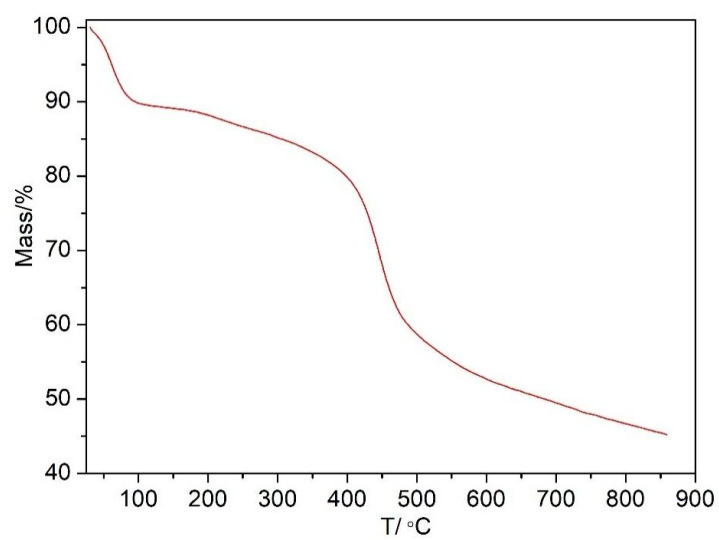


Figure S29. Thermogravimetric curve of **mMOF-1**.

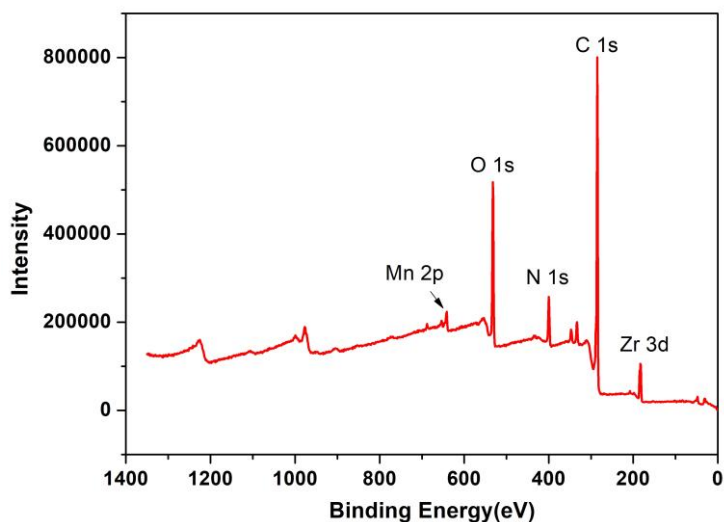


Figure S30. XPS analysis spectra of Zr-Mn-PCN.

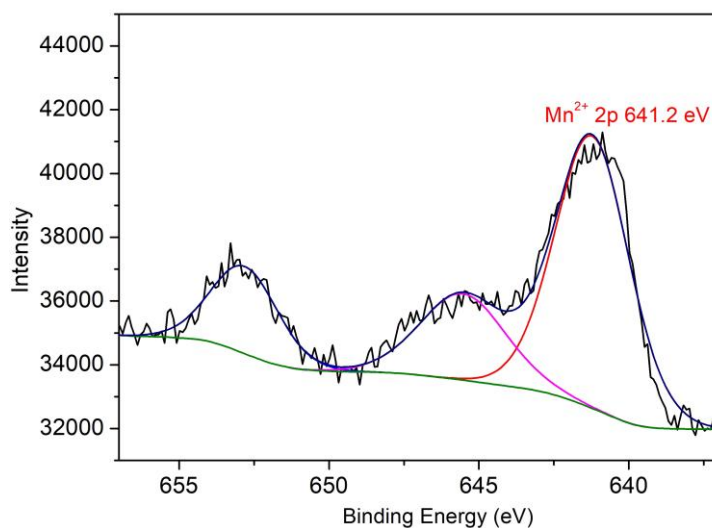


Figure S31. High resolution XPS spectrum of Mn 2p.

7. Reference

1. W. Nie, D. E. Tarnopol, C. C. L. McCrory. *J. Am. Chem. Soc.* **2021**, *143*, 10, 3764-3778.
2. O.V. Dolomanov, L.J. Bourhis, R. J. Gildea, J. A. K. Howard, H. Puschmann. *J. Appl. Cryst.* **2009**, *42*, 339-341.
3. A. L. Spek, *Acta Cryst.*, **2015**, *C71*, 9-18.
4. W. Gong, Y. Xie, X. Wang, K. O. Kirlikovali, K. B. Idrees, F. Sha, H. Xie, Y. Liu, B. Chen, Y. Cui, O. K. Farha, *J. Am. Chem. Soc.* **2023** *145*, 2679-2689.
5. D. Feng, Z.-Y. Gu, J.-R. Li, H.-L. Jiang, Z. Wei, H.-C. Zhou, *Angew. Chem. Int. Ed.* **2012**, *51*, 10307-10310.
6. D. Feng, W.-C. Chung, Z. Wei, Z.-Y. Gu, H.-L. Jiang, Y.-P. Chen, D. J. Darensbourg, H.-C. Zhou, *J. Am. Chem. Soc.* **2013**, *135*, 17105-17110
7. T. C. Wang, W. Bury, D. A. Gómez-Gualdrón, N. A. Vermeulen, J. E. Mondloch, P. Deria, K. Zhang, P. Z. Moghadam, A. A. Sarjeant, R. Q. Snurr, J. F. Stoddart, J. T. Hupp, O. K. Farha, *J. Am. Chem. Soc.* **2015** *137*, 3585-3591.